



Proceeding Paper

A Predator-Prey Model from Collective Dynamics and Self-Propelled Particles Approach [†]

Yaya Youssouf Yaya ^{1,2}

¹ Université Assane Seck de Ziguinchor, Ziguinchor 27000, Senegal; yy.y@zig.univ.sn

² École Normale Supérieure de N'djaména, Tchad

[†] Presented at the 1st International Online Conference on Mathematics and Applications; Available online: <https://iocma2023.sciforum.net/>

Abstract: The definition and description of the dynamics of predator-prey system consists in one of the fundamental problems of the population biology. Since 1925, several models have been introduced. Although they are highly effective, most of them neglect certain relevant criteria such as the spatial and temporal distribution of the studied species. We introduced these criteria by coupling two models designed initially for collective dynamics. The first is for predators mobility, a Vicsek type model and the second is a Brownian Particle (BP) model for prey. We observed, as naturally in the classical models, periodic cycles of the density of predators and prey. In this case, the period of oscillations depends relatively on the collective dynamics parameters.

Keywords: collective behavior; self-propelled particles; brownian particles; predator-prey; reaction-diffusion; limit cycle

1. Introduction

The study of population dynamics is a subject of multidisciplinary research involving ecology, biology, mathematics and physics. It's sometimes oriented specifically in the dynamics of two species: Predators and Prey. In this perspective, the model developed independently by A. J. Lotka (1925) [1] and V. Volterra (1926) [2] provides a satisfactory explanation of the observed phenomena such as the periodic variation in species density.

Since then, several variants of this model (called LV) are derived. They are discrete or continuous dynamical systems whose qualitative study most often shows the existence of a steady state and periodic solutions around it [3,4]. Some variants of these models incorporate the mobility (spatio-temporal distribution) of the studied species, they are known as reaction-diffusion systems [5]. The common point between the above-mentioned approaches is that they are Eulerian and deterministic and known as the mean-field approach. There is still some stochastic formulations studied in [6,7].

Recently, Agent Based Model (ABM) are also used to interpret predator-prey dynamics [8]. This concept was first introduced to study the collective behavior of a given species. These are the Self Propelled Particles Models (SPP) ; they are presented in two or three-dimensional space by an extensive investigation[9–13]. Central issues here include the mechanisms by which autonomous agents interact to exhibit emergent collective behavior and the properties of the resulting behavior. On the other hand, the mobility of certain species such as bacteria or phytoplankton is not a coherent collective dynamic but rather a random walk. Individuals from these species are generally considered as Brownian Particles (BP) [14–16]. In sum, Self-Propelled Particles Models are introduced to study the collective dynamics of a single species but never considered for the simultaneous description of two species ; Less so for two species of Predator-Prey. If so, what about the basic properties deduced from these models such as orientation ordering, cluster formation etc.?

Our approach consists in constructing a framework interpreting a Predator-Prey's type of dynamics. Individuals are considered as material points inside the domain: a periodic



Citation: Yaya, Y.Y. A Predator-Prey Model from Collective Dynamics and Self-Propelled Particles Approach. *Comput. Sci. Math. Forum* **2023**, *1*, 0. <https://doi.org/>

Academic Editor: Firstname
Lastname

Published: 28 April 2023



Copyright: © 2023 by the author. Licensee MDPI, Basel, Switzerland. This article is an open access article distributed under the terms and conditions of the Creative Commons Attribution (CC BY) license (<https://creativecommons.org/licenses/by/4.0/>).

box of size $B \times B$ located by their positions on the Cartesian plane and animated with some velocity.

To implement this approach, we develop in the first section two separate models to simulate mobility of prey and predators. For this purpose, we use the SPP and BP models respectively. Then, we mix the two with assumptions of living interactions to illustrate via flowchart and equations a prey-predator type dynamics. We make then a python program to incorporate the global model.

Throughout the analysis of this model, we look for a range of standard parameters for which periodic oscillations between the densities of species can be found. This is followed by an underlying analysis of the characteristics of a collective behavior.

2. Models and Simulation Setting

We designed separately prey and predator model describing their motions. Then we added Predator-Prey model which take in account their living interactions.

2.1. Prey's Motion

For prey motion, n_p particles are randomly uniformly distributed inside the domain, their density by unit area is $\rho_p = n_p/B^2$. $r_p^i(t), v_p^i(t)$ represent respectively, the position and velocity of particle i at time t where the index p is set for prey. A complex type of this models using thrust force and interactions between particles is studied in [16].

In the beginning of the simulation ($t = 0$), we set prey's velocities from a Gaussian distribution with zero mean and σ standard deviation (i.e., each particle has a random normal velocity from $[-3\sigma, 3\sigma]$; $\sigma = \frac{1}{3}$ is chosen to have values in $[-1, 1]$). After the first time step, each particle undergoes the action of a total force $M \frac{dv_p^i}{dt}$ that denoted F^i and moves according to Langvin Equation (1) [16]

$$M \frac{dv_p^i}{dt} = F^i(t) = -\gamma v_p^i(t) + R^i(t), \tag{1}$$

where, M is the mass of prey, is set to 1 for simplicity ; v_p^i the velocity of prey i ; γ is the coefficient of viscous friction, which is set by the properties of the environment and the particle geometry; $R^i(t)$ is a random force given by: $R^i(t) = \sqrt{2\gamma k_B T} \zeta^i$, with k_B, T and ζ^i are respectively the Boltzmann constant, temperature and Gaussian white noise with zero-mean and unit variance. $T_B = k_B T$ is called Boltzmann temperature. We used Box-Muller transformation to compute the components of ζ^i , it consists in choosing two elements u_1 and u_2 from a uniform distribution from $]0, 1]$ and mapping them to two standard, normally distributed samples: $\zeta_x^i = \sqrt{-2 \log(u_1)} \cos(2\pi u_2)$, $\zeta_y^i = \sqrt{-2 \log(u_1)} \sin(2\pi u_2)$. Thus, we used Verlet algorithm to perform prey's position and Störmer-Verlet method for their velocities. (Cf. [17]) $r_p^i(t + \tau) = 2r_p^i(t) - r_p^i(t - \tau) + \tau^2 F^i(t)$, $v_p^i(t) = \frac{r_p^i(t+\tau) - r_p^i(t-\tau)}{2\tau}$ In this system, each particle has a Brownian trajectory (random walk) and the average velocity of all particles depends closely on two parameters γ and T_B (Cf. additional materials).

Table 1. Global and predator parameters.

(a) Summary of global parameters and that used in the prey model. Standard values are used for simulation			
Name	Standard Values	Description	Fields (Unit)
GLOBALES VARIABLES			
B	125	Length of domain	\mathbb{R}^* (mm)
L_t	5×10^5	Number of time steps	\mathbb{N}^* (s)
τ	1	Time step	\mathbb{R}^* (s)
PARAMETERS OF PREY MODEL			
ρ_q	0.12	Density in number by unit area	$[0.01; 4]$ (mm^{-2})
γ	0.2	Coefficient of viscous friction	\mathbb{R}^* (N)
T_B	0.01	Boltzmann Temperature	\mathbb{R}^* (J)
(b) Parameters of Predator model			
Name	Standard Values	Description	Fields (Unit)
η	0.09	Noise strength	$[0; 1]$ (1)
ρ_p	0.012	Density in number by unit area	$[0.01; 1](\text{mm}^{-2})$
R_r	1	Radius of repulsion zone (zor)	$[0; L]$ (mm)
R_a	4	Radius of alignment zone (zoa)	$[0; L]$ (mm)
v_q^o	0.5	Constant speed of any particle	$[0; R_r]$ (1)
α	π	Angle of perception	$[0; 2\pi]$ (rad)

2.2. Predator’s Motion

To describe predator’s motion in the domain, we used a variant of Vicsek model and added a repulsion rule (Cf. [9,12,18]). So, n_q predator-particles are distributed inside the domain and move with a constant speed v_q^o ; Their density is $\rho_q = n_q / B^2$ and $r_q^i(t), v_q^i(t)$ represent respectively position and velocity vectors for i^{th} particle at time t where subscript q denote predator. For initial conditions, we set to each particle, a uniform random position $r_q^i(0)$ and velocity $v_q^i(0)$ (Cf. [16]). Then, in any time step τ , the position $r_q^i(t)$ changes according to Equation $r_q^i(t + \tau) = r_q^i(t) + \tau v_q^i(t)$, and the velocity v_q^i depends on the position of the i^{th} particle which is either in the area of repulsion (zor) or alignment (zoa). These areas are defined by circles whose radii are noted R_r for zor and R_a for zoa with $R_r < R_a$. The first behavioral zone, represented by a circle of smaller radius R_r , is responsible for the maintenance of a minimum distance between neighboring particles, while the second one with a grater radius R_a is used for aligning the particle velocities (Figure 1a).

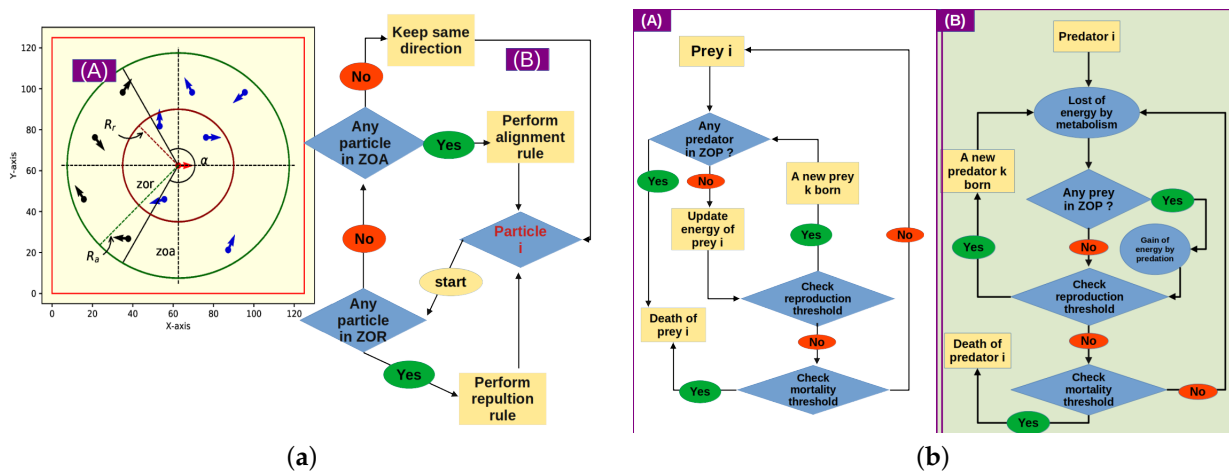


Figure 1. Diagram of interactions. (a): (A) Schema of interactions between particles in the Vicsek-type model. The central particle (red arrow) turns away from the nearest neighbors (blue arrows) within the zone of repulsion (the inner circle of radius R_r , zor) to avoid collisions and aligns itself with the neighbors (blue arrows) within the zone of alignment (the outer circle of radius R_a , zoa). The alignment exclude particles (black arrows) within blind angle $(2\pi - \alpha)$; $\alpha = 4.19\text{rad}$ [13]. (B) Flowchart illustrating movement choices of a predator i . (b): Flowchart illustrating living interaction between preys (A) and predators (B). ZOP denote zone of predatory and the equations satisfying the different conditions are shown in the underlying section.

In the same figure, we put flowchart illustrating movement choices of a predator i whose rules are described as follows:

(a) Repulsion rule: If there are n_r neighbors around i in zor, the velocity $v_q^i(t + \tau)$ is given by Equation. $v_q^i(t + \tau) = R(\xi_i(t))V_r^i(t)$, with $V_r^i(t)$ the desired direction of particle i is given by Equation $V_r^i(t) = -v_q^o \sum_{j \neq i}^{n_r} r_q^{ij}(t) / \left| \sum_{j \neq i}^{n_r} r_q^{ij}(t) \right|$, where v_q^o is a constant speed for all particles; $r_q^{ij} = r_q^j - r_q^i$ is the vector in the direction of neighbor j and $R(\xi_i(t))$ is the rotation matrix. $\xi_i(t)$ is a random angular noise obtained from $[-2\pi\eta; 2\pi\eta]$ by Gaussian-distribution, where $\eta \in [0; 1]$ represents the noise strength. The standard deviation is then around $\frac{2\pi}{3}\eta$.

(b) Alignment rule: If there are no neighbors in the zone of repulsion, the individual i responds to others which are in the zone of alignment with:

$$v_q^i(t + \tau) = \begin{cases} R(\xi_i(t))V_a^i(t), & b > a \\ v_q^i(t)v_q^o, & b \leq a \end{cases} \quad (2)$$

where: b is the cosine of the angle measured between $v_q^i(t)$ and r_q^{ij} ; It's evaluated to check if particle i see particle j ; $a \in [-1; 0]$ has a fixed value which is the cosine of half angle of perception α , the blind angle should be $360^\circ - \alpha$. Thus, if $a = -1$, central particle i interact with all particles inside zone of alignment. The desired direction of particle i in zoa is $V_a^i(t) = v_q^o \phi(t)^\lambda \sum_{j=1}^{n_a} v_j^f(t) / \left| \sum_{j=1}^{n_a} v_j^f(t) \right|$, with n_a is the number of particles in the zone of

alignment and $\phi(t)$ the polar order (or polarization) given by: $\phi(t) = \frac{1}{n_a} \left| \sum_{i=1}^{n_a} v_q^i(t) \right|$; and λ is the degree of polarization.

(c) Absolute rule: If repulsion happens, the alignment is neglected.

(d) Alternative rule: If there are no individuals in the both zones, the particle i keeps its previous direction thus, $v_q^i(t + \tau) = v_q^i(t)v_q^o$.

Finally, the parameters involved in this model for predators are shown in Table 2. Thus, in the next section, we will model the vital interactions simulating a prey-predator dynamic.

Table 2. Parameters of Predator model/

Name	Standard Values	Description	Fields (Unit)
η	0.09	Noise strength	[0; 1] (1)
ρ_p	0.012	Density in number by unit area	[0.01; 1] (mm^{-2})
R_r	1	Radius of repulsion zone (zor)	[0; L] (mm)
R_a	4	Radius of alignment zone (zoa)	[0; L] (mm)
v_q^o	0.5	Constant speed of any particle	[0; R_r] (1)
α	π	Angle of perception	[0; 2π] (rad)

2.3. The Predator-Prey Model

In addition to previous models describing movement of prey and predator (Sections 2.1 and 2.2), we interested in this part on their dynamic of evolution as two species living in a common environment (the domain). To describe this dynamic, we introduced a Predator-Prey model by coupling those two models through underline assumptions.

Firstly, we treated prey as living agents with the principle idea that any prey has some energy state which varies according to its position towards predators. It features life states of all individuals: survival, reproduction and mortality. Then, at $t = 0$, we set $n_p(0)$ the initial size of prey population and an initial energy $E_p^i(0)$ to each one. It's a random value gotten from Gaussian distribution with zero mean and σ_{E_p} standard deviation (i.e., $E_p^i(0) \hookrightarrow \mathcal{N}(0, \sigma_{E_p})$).

Therefore, after each time step, i^{th} prey survive when it's outside the predatory area of all predators (Equation ??). It gains a *survival bonus*, an energy E_{s_p} which can increase or decrease its next state of energy, this modeling the fact that each prey can survive by engendering or not another one or just die. $\forall j \quad |r_i^p(t) - r_j^f(t)| > R_p$, thus $E_p^i(t + \tau) = E_p^i(t) + E_{s_p}$. Consequently, if the energy state reach some certain *reproduction threshold* E_{r_p} , the individual will be able to reproduce by cloning. Then a new prey k born inside a birth zone (zob_p) of radius R_{b_p} ; he inherits from his ancestor the similar movement abilities $E_p^i(t + \tau) \geq E_{r_p} \Rightarrow i^{th}$ prey clone. Subsequently, its mortality is due to predatory or deficiency of energy, it happens when the energy become less than a fixed *mortality threshold* E_{d_p} , $E_p^i(t) \leq E_{d_p} \Rightarrow i^{th}$ prey die.

With the same order of ideas, we approached in second instance the dynamics of predators. Thus, for an initial size of population $n_q(0)$, we assumed that predator will need energy to survive, it's also a normal distribution $E_q^i(0)$ with zero mean and σ_{E_q} standard deviation.

Therefore, in each time step, it uses E_{m_q} amount of energy for metabolism (2). It's deriving energy come from predation of preys present in it's zone of predatory zop (a circle of radius R_p). Thus, its state of energy decrease by the *metabolism cost* E_{m_q} or increase by the *predatory bonus* E_{a_q} , $E_q^i(t + \tau) = E_q^i(t) - E_{m_q}; |r_i^f(t) - r_j^p(t)| \leq R_p \Rightarrow E_q^i(t + \tau) = E_q^i(t) + E_{a_q}$.

Following this energy update, predator dies when it's state of energy decrease below the *mortality threshold* E_{d_q} . Otherwise, if its energy level reaches more than the *reproduction threshold* E_{r_q} , a new predator k born with a random normal energy $E_q^k(t + \tau) \hookrightarrow \mathcal{N}(0, \sigma_{E_q})$ and random uniform velocity inside the zone of birth (zob_q) of radius R_{b_q} . This is the cloning reproduction principle that we used for prey $E_q^i(t) \leq E_{d_q} \Rightarrow i^{th}$ predator die, $E_q^i(t + \tau) \geq E_{r_q} \Rightarrow i^{th}$ predator clone.

Finally, after recap on Table 3, the parameters involved in the model described above, we designed a python program for simulations. The files are available on this [link](#) where "main.py" generates the data and "anim.py" simulates interactions between the species.

Table 3. Parameters of Predator-Prey model ; standard values are those which systemics a pseudo-periodic regime.

Name	Standard Values	Description	Fields (Unit)
PREYS			
R_{b_p}	0.5	Zone of birth's radius (zob_p)	$[0; L]$ (mm)
σ_{E_p}	2.73	Standard deviation of energy distribution	\mathbb{R}^* (1)
E_{r_p}	6	Reproduction threshold	\mathbb{R}^* (J)
E_{s_p}	$\mathcal{N}(0, \sigma_{E_p})$	Survival bonus	\mathbb{R}^* (J)
E_{d_p}	-8	Mortality threshold	\mathbb{R}^* (J)
PREDATORS			
R_p	6	Zone of predatory's radius (zop)	$[0; L]$ (mm)
R_{b_q}	1	Zone of birth's radius (zob_q)	$[0; L]$ (mm)
σ_{E_q}	2.73	Standard deviation of energy distribution	\mathbb{R}^* (1)
E_{m_q}	0.01	Metabolism cost	\mathbb{R}^* (J)
E_{a_q}	0.025	Predatory bonus	\mathbb{R}^* (J)
E_{r_q}	8	Reproduction threshold	\mathbb{R}^* (J)
E_{d_q}	-8	Mortality threshold	\mathbb{R}^* (J)

3. Results And Discussion

We performed computer simulations to analyze the predator-prey model. Unless explicitly stated, we kept all parameters standard as indicated in Table 1. *Standard parameters* provide a regime where the density of species oscillates over time, a pseudo-periodic regime for all trials done. However, by varying certain parameters, one can have other types of regime like the simultaneous extinction of two species or the survival of one and the extinction of the other.

We started to run ones the model by focusing mainly on three characteristics time in $[3 \times 10^3, 8 \times 10^3]$. The choice of characteristic time is with respect to predator density as: $(\rho_{q_{min}} \leftarrow t_{min}), (\rho_{q_{mid}} \leftarrow t_{mid}), (\rho_{q_{max}} \leftarrow t_{max})$ where subscripts *min*, *mid*, and *max* denote respectively the minimum, middle and maximum densities. Not that in this notation t_{min} might be greater than t_{max} etc., because subscripts here are only rigorously attached to density values. These three cases typically represent the different phases of predators collective dynamics. In this sense, we illustrated the spatial distribution of species on Figure 2A snapshots (a-c); i.e., the locations inside the domain of predators (blue) and preys (orange) at specific time ($t_{min}, t_{mid},$ or t_{max}). We noticed that prey density is less important where that of predators is elevated and vice versa, such a fact gives the intuition to cyclic evolution of species which is represented in Figure 2A(d). For hole experience, we recorded the range of densities for predators and prey respectively in $[0.089, 0.25]$ and $[0.29, 0.89]$. The corresponding characteristics densities are $(\rho_{q_{min}}, \rho_{q_{mid}}, \rho_{q_{max}}) = (0.089, 0.21, 0.25)$. Hence, we observed that density variations have an impact on the collective dynamics notably on the particle orientation ordering and cluster formation groups ; this results is also found in many study of Viscek-type models.

For this, we investigated particle orientation ordering by evaluating polar order parameter $\Phi(t)$, which quantifies the alignment of predator particles to the average instantaneous velocity vector $\Phi(t) = \frac{1}{n_q(t)v_q^0} \left| \sum_{i=1}^{n_q(t)} v_q^i(t) \right|$; this parameter goes from zero in the case of a disordered phase to one in the case of a completely ordered phase. We have shown on

Figure 2A(e) the evolution of polar order parameter $\Phi(t)$ where particles seem less orderly at low density. Anyway, it's not obvious to find a correlation between the variation of particles density and their polar order parameter because the appearance of newborns disturbs alignment of particles, and we observe emergence of a spontaneous local phase transition.

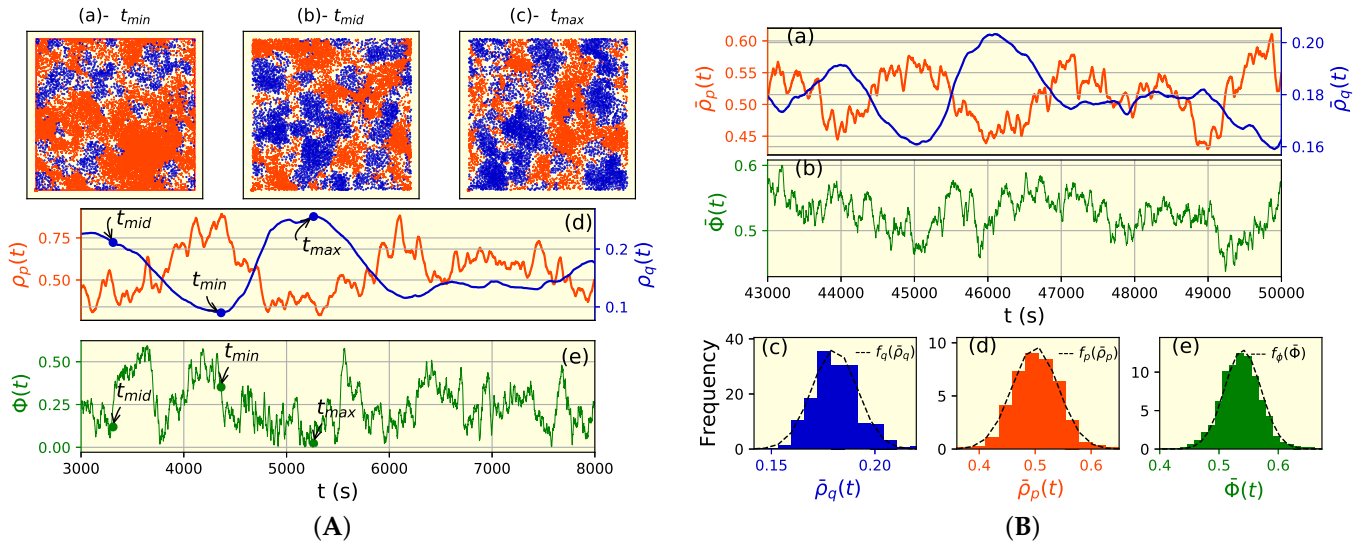


Figure 2. Snapshots of particles and related indicators. **(A)** Snapshots of particles distribution in the domain: predators (blue) and prey (brown) respectively for three cases of predator density: (a) Minimum density $\rho_{q_{min}} = 0.10$; (b) Maximum density $\rho_{q_{max}} = 0.20$ and (c) Middle density $\rho_{q_{mid}} = 0.18$. **(B)** Sub-figures (d,e) show respectively the density evolution of spices and the polar order parameter $\Phi(t)$ (green) versus time. t_{min} , t_{mid} and t_{max} indicate the three Cases mentioned above. (a) Average density evolution of predators $\bar{\rho}_q(t)$ (blue) and prey $\bar{\rho}_p(t)$ (brown) (b) the corresponding average polar order parameter $\bar{\Phi}(t)$ (green). The average is taken from 18 independent runs within standards parameters except total time equal to $5 \cdot 10^4$. Sub-figures (c–e) show respectively the distribution of $\bar{\rho}_q(t)$, $\bar{\rho}_p(t)$ and $\bar{\Phi}(t)$; Thus, dashed lines are the corresponding fitted function f_q , f_p , and f_Φ (see Equations ??, ??, ??).

To more understand the evolution of predator-prey densities ($\rho_q(t), \rho_p(t)$) and the equivalent predator polar ordering ($\Phi(t)$), we run 18 trials with total time $L_t = 5 \times 10^4$. Results are like a same i.e., the density of predators $\rho_q(t)$ oscillate in $[0.013; 0.33]$ and that of preys $\rho_p(t)$ in $[0.12; 1.32]$. It results as on the first trial that $\rho_q(t)$ increase when $\rho_p(t)$ decrease and vice versa. Thus, there is an equilibrium point ($\bar{\rho}_q(t), \bar{\rho}_p(t)$) and limit cycle around it. We also highlighted that the curve of ρ_q is smoother than the curve of ρ_p , this is due to the height impact of randomness in prey dynamic assumptions. This randomness effect appears also on polar order parameter $\Phi(t)$ which is bounded in $[0.076, 0.67]$. Therefore, predators could be completely disordered some time, and they cannot reach a degree of order more than 0.67. This indicates that the presence of preys has an impact on predator collective dynamic as disordering factor.

We continued our analysis by looking at histograms of ($\bar{\rho}_q(t), \bar{\rho}_p(t), \bar{\Phi}(t)$) which denote the instantaneous average (quadratic mean) of ($\rho_q(t), \rho_p(t), \Phi(t)$) where $t \in [4.3 \times 10^4, 5 \times 10^4]$. We found approximate functions f_q, f_p and f_Φ to, fit respectively predator and prey density distribution and polar order parameter distributions (sub-figures (c–e) from Figure 2) $f_q(\bar{\rho}_q(t)) = \mathcal{N}(\mu_q, \sigma_q) = \mathcal{N}(0.18, 0.011)$; $f_p(\bar{\rho}_p(t)) = \mathcal{N}(\mu_p, \sigma_p) = \mathcal{N}(0.5, 0.041)$; $f_\Phi(\bar{\Phi}(t)) = \mathcal{N}(\mu_\Phi, \sigma_\Phi) = \mathcal{N}(0.54, 0.31)$.

Since only the evolution of the predator density does not follow a Gaussian distribution, we interested on fluctuation in the number of predator particles in the system: $\langle \Delta n_q(l) \rangle = \sqrt{\langle n_q(l)^2 \rangle - \langle n_q(l) \rangle^2}$ where $n_q(l)$ denotes the number of predators in a box of linear size l . $\langle \Delta n_q(l) \rangle$ is in general proportional to $\langle n_q(l) \rangle^\beta$. $\beta = 0.5$ correspond to normal

fluctuation while $\beta \approx 0.5$ is the giant fluctuation. In our system, the number fluctuation of predator particle is estimated for three density case, for minimum and middle densities, the critical exponent is $\beta \approx 0.8$; this corresponds to giant fluctuation. For maximum density, the fluctuation is normal because of $\beta \approx 0.5$ (Figure 3a).

We examined finally cluster distribution of predator particle. Formally, the cluster dynamics of the SPP system can be described by deriving a master equation for the evolution of the probability $p(m)$, where $m = m_1, m_2, \dots, m_N$ with m_1 being the number of isolated particles, m_2 the number of two-particle clusters, m_3 the number of three-particle clusters etc. Cluster in our model is defined as a group of particles with a distance between neighbors smaller or equal to the radius of alignment zone R_a , i.e., particles interacting directly or via neighboring agents are included into one cluster ([13]).

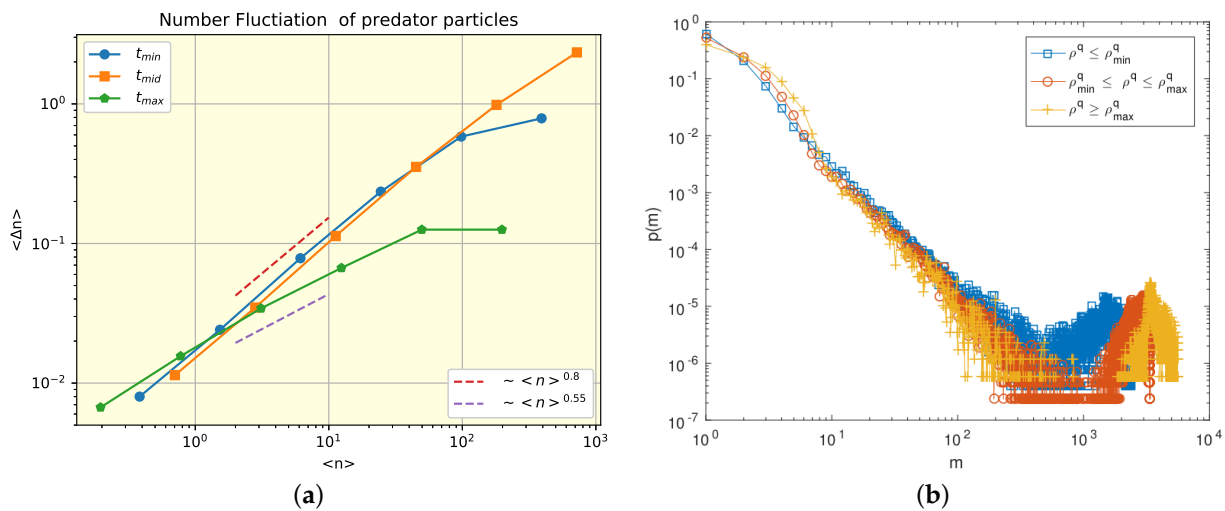


Figure 3. Number fluctuation and cluster statistics. (a) Number fluctuation of predator particle for three characteristic time: at minimum density t_{min} , middle density t_{mid} and maximum density t_{max} . The critical exponent β is in $[0.55; 0.8]$. (b) Cluster statistics for three range of predator density. $\rho^q \leq \rho_{q_{min}}^q, \rho_{q_{min}}^q \leq \rho^q \leq \rho_{q_{max}}^q, \rho^q \geq \rho_{q_{max}}^q$. $\rho_{q_{min}}^q = 0.16$ and $\rho_{q_{max}}^q = 0.21$. $L_t = 10^5$ and the rest of parameters are standard.

4. Conclusions

In summary, we built a predator-prey model from collective dynamics and self-propelled particles approach. Despite the plethora of assumptions, the stability of the system is possible with the admissible parameters which gives a quasi-periodic regime.

The main results related to SPP & BP models are kept with the particularity that the densities are dynamic here. Let us note however the difficulty in the design of the algorithm caused by the large size of parameters.

Funding:

Institutional Review Board Statement:

Informed Consent Statement:

Data Availability Statement:

Acknowledgments: This paper and the research behind it would not have been possible without the exceptional support of M. Romensky and David J. T Sumpter from Uppsala University. Their enthusiasm, knowledge and exacting attention to detail have been an inspiration and kept my work on track from my first visit in their Lab to the final draft of this paper.

Conflicts of Interest:

References

1. James Lotka, A. *Elements of Physical Biology*; Williams & Wilkins Company: Baltimore, MD, USA, 1925; p. 460.
2. Voterra, V. Fluctuations in the abundance of a species considered mathematically. *Nature* **1926**, *118*, 558–560.
3. May, R.M. Limit Cycle in Predator-Prey Communities. *Science* **1972**, *177*, 900–902.
4. Arditi, R.; Ginzburg, L.R. Coupling in Predator-Prey Dynamics: Ratio-Dependence. *J. Theor. Biol.* **1989**, *139*, 311–326.
5. Ainseba, B.; Bendahmane, M.; Noussair, A. A reaction–diffusion system modeling predator–prey with prey-taxis. *Nonlinear Anal. Real World Appl.* **2008**, *9*, 2086–2105.
6. Rodrigues, A.L.; Tomé, T. Reaction-diffusion stochastic lattice model for a predator-prey system. *Braz. J. Phys.* **2008**, *38*, 87–93.
7. Liu, M.; Fan, M. Permanence of Stochastic Lotka–Volterra Systems. *J. Nonlinear Sci.* **2017**, *27*, 425–452.
8. Lin, Y.; Abaid, N. Collective behavior and predation success in a predator-prey model inspired by hunting bats. *Phys. Rev. E* **2013**, *88*, 062724.
9. Vicsek, T.; Czirók, A.; Ben-Jacob, E.; Cohen, I.; Shochet, O. Novel Type Of phase Transition in a System of Self-Driven Particles. *Phys. Rev. Lett.* **1995**, *75*, 1226–1229.
10. Sumpter, D.J.T. The principles of collective animal behaviour. *Phil. Trans. R. Soc. B* **2006**, *361*, 5–22.
11. Buhl, J.; Sumpter, D.J.T.; Couzin, I.D.; Hale, J.J.; Despland, E.; Miller, E.R.; Simpson, S.J. From Disorder to Order in Marching Locusts. *Science* **2006**, *312*, 1402–1406.
12. Vicsek, T.; Zafeiris, A. Collective motion. *Phys. Rep.* **2012**, *517*, 71–140.
13. Romenskyy, M.; Lobaskin, V. Statical properties of swarms of self-propelled particles with repulsions across the order-disorder transition. *Eur. Phys. J. B* **2013**, *86*, 91.
14. Ebeling, W.; Schweitzer, F.; Tilch, B. Active Brownian particles with energy depots modeling animal mobility. *BioSystems* **1999**, *49*, 17–29.
15. Romanczuk, P.; Bär, M.; Ebeling, W.; Lindner, B.; Schimansky-Geier, L. Active Brownian particles. *Eur. Phys. J. Spec. Top.* **2012**, *202*, 1–162.
16. Lobaskin, V.; Romenskyy, M. Collective dynamics in system of Brownian particles with dissipative interactions. *Phys. Rev. E* **2013**, *87*, 052135.
17. Verlet, L. Computer “Experiments” on Classical Fluids. I. Thermodynamical Properties of Lennard-Jones Molecules. *Phys. Rev. E* **1967**, *159*, 98.
18. Cousin, I.D.; Krause, J.; James, R.; Ruxton, G.D.; Franks, N.R. Collective memory and spatial sorting in animal group. *J. Ther. Biol.* **2002**, *218*, 1–11.

Disclaimer/Publisher’s Note: The statements, opinions and data contained in all publications are solely those of the individual author(s) and contributor(s) and not of MDPI and/or the editor(s). MDPI and/or the editor(s) disclaim responsibility for any injury to people or property resulting from any ideas, methods, instructions or products referred to in the content.